Enhanced orbital fluctuations in Mg-doped MnV_2O_4 single crystals

Qing-Yuan Liu,[1] Zi-Yi Liu,[1,2] Xue-Bo Zhou,[1] Takeshi Yajima,[3] Yoshiya Uwatoko,[3] Jin-Guang Cheng,[2,4] Lei Tao,[5] Zhi-Guo Liu,[1] Ming-Xue Huo,[5,*] Xian-Jie Wang,[1,†] and Yu Sui[1,5,‡]

[1]*School of Physics, Harbin Institute of Technology, Harbin 150001, China*
[2]*Beijing National Laboratory for Condensed Matter Physics and Institute of Physics, Chinese Academy of Sciences, Beijing 100190, China*
[3]*Institute for Solid State Physics, The University of Tokyo, Kashiwanoha 5-1-5, Kashiwa, Chiba 277–8581, Japan*
[4]*Songshan Lake Materials Laboratory, Dongguan, Guangdong 523808, China*
[5]*Laboratory for Space Environment and Physical Sciences, Harbin Institute of Technology, Harbin 150001, China*

(Received 14 October 2019; published 19 December 2019)

We investigated the magnetic and structural transitions of $Mn_{1-x}Mg_xV_2O_4$ ($x = 0$, 0.05, 0.1, 0.15) single crystals with a normal spinel structure. These crystals all exhibit a cubic-to-tetragonal structural transition at T_S caused by the orbital ordering of V^{3+} ions, which is followed by a ferrimagnetic ordering transition at T_M. We found that T_M is equal to T_S for $x \leqslant 0.1$, but the ferrimagnetic transition is shifted to lower temperature by Mg doping and T_S and T_M can be separated clearly for $x = 0.15$. Moreover, a certain degree of orbital fluctuations was brought about by the ferrimagnetic transition at T_M, but suppressed below T^*, leading to another transition from weak orbital fluctuations to further orbital ordering at T^*. The orbital fluctuations were caused by the anomalous interchain interaction J^c and can be also enhanced by the substitution of Mg for Mn due to the decrease of the distance between V^{3+} ions along the c direction ${}^cR_{\text{v-v}}$, which results in the increase of J^c.

DOI: 10.1103/PhysRevB.100.224418

I. INTRODUCTION

Transition-metal vanadium oxides with normal spinel structure (AB_2O_4) have attracted considerable interest because of some intriguing physical phenomena, such as orbital ordering, geometrical frustration, and multiferroicity [1–4]. The V^{3+} ion in AV_2O_4 occupies the B site forming a geometrically frustrated pyrochlore lattice and can form orbital ordering at low temperature [5–10]. Accompanying the orbital ordering, AV_2O_4 usually undergoes a cubic-to-tetragonal structural transition, which partially releases the geometrical frustration and then leads to a long-range magnetic ordering [3,11,12]. Due to the intricate coupling among the orbital, spin, and lattice degrees of freedom, there are complex magnetic and structural transitions in some normal spinel AV_2O_4 (A = Mn, Fe, Co) [11–14].

MnV_2O_4 was usually reported to undergo two successive phase transitions at $T_S \sim 56$ K and $T^* \sim 52$ K, respectively [14–18]. In the early reports, it was believed that a magnetic ordering transition first occurs at T_S, and then a structural transition from the cubic to the tetragonal phase is induced by orbital ordering at T^*, accompanied with a collinear to noncollinear ferrimagnetic transition [15–17,19]. However, in recent years, some different viewpoints about the origin of these two transitions have been put forward. By using thermal expansion and variable temperature x-ray-diffraction (XRD) measurements, Suzuki *et al.* pointed out that the orbital ordering and structural transition first takes place at T_S, accompanied with a non-collinear ferrimagnetic ordering [7], but they have found no extra transition at T^*. In addition, Myung-Whun *et al.* also argued that a structural transition and a ferrimagnetic ordering occur simultaneously at T_S based on the specific-heat and magnetic susceptibility measurements [14]. Nevertheless, many recent papers still supported that the ferrimagnetic ordering happens at a higher temperature than the structural transition temperature [20–23]. Thus, the nature of these two transitions of MnV_2O_4 remains under debate.

In addition, the pattern of orbital ordering in MnV_2O_4 is also highly controversial. Suzuki *et al.* proposed an A-type antiferro-orbital ordering via analyzing the XRD of MnV_2O_4 single crystal below T_S [7], but Chung *et al.* found that the ferro-orbital ordering should be more stable because the interchain exchange interaction is a strong antiferromagnetic interaction [24]. Garlea and Chung *et al.* also observed a spin-wave gap arising around T^* [17,25], indicating the existence of single-ion anisotropy. Such a magnetic anisotropy may be a consequence of the unquenched orbital moment of the V^{3+} ion, in support of an uncompleted orbital ordering in MnV_2O_4. Therewith, Myung-Whun *et al.* further guessed the existence of orbital fluctuations below T^* in MnV_2O_4 [14]. These results indicate that the orbital state in MnV_2O_4 is very complex, and it is closely related to the transition at T^*. Due to the coupling between orbitals and lattice, the phonons would be scattered by fluctuating orbitals, which results in positive temperature dependence of phonon thermal conductivity [16,26,27]. By contrast, the phonon thermal conductivity would be enhanced with decreasing temperature after orbital ordering. Therefore, the thermal conductivity can be an effective tool to detect the orbital fluctuations indirectly.

In a Mott insulator like MnV_2O_4, an orbital ordering determines sign of the superexchange interaction between spins.

*Corresponding author: huomingxue@hit.edu.cn
†Corresponding author: wangxianjie@hit.edu.cn
‡Corresponding author: suiyu@hit.edu.cn

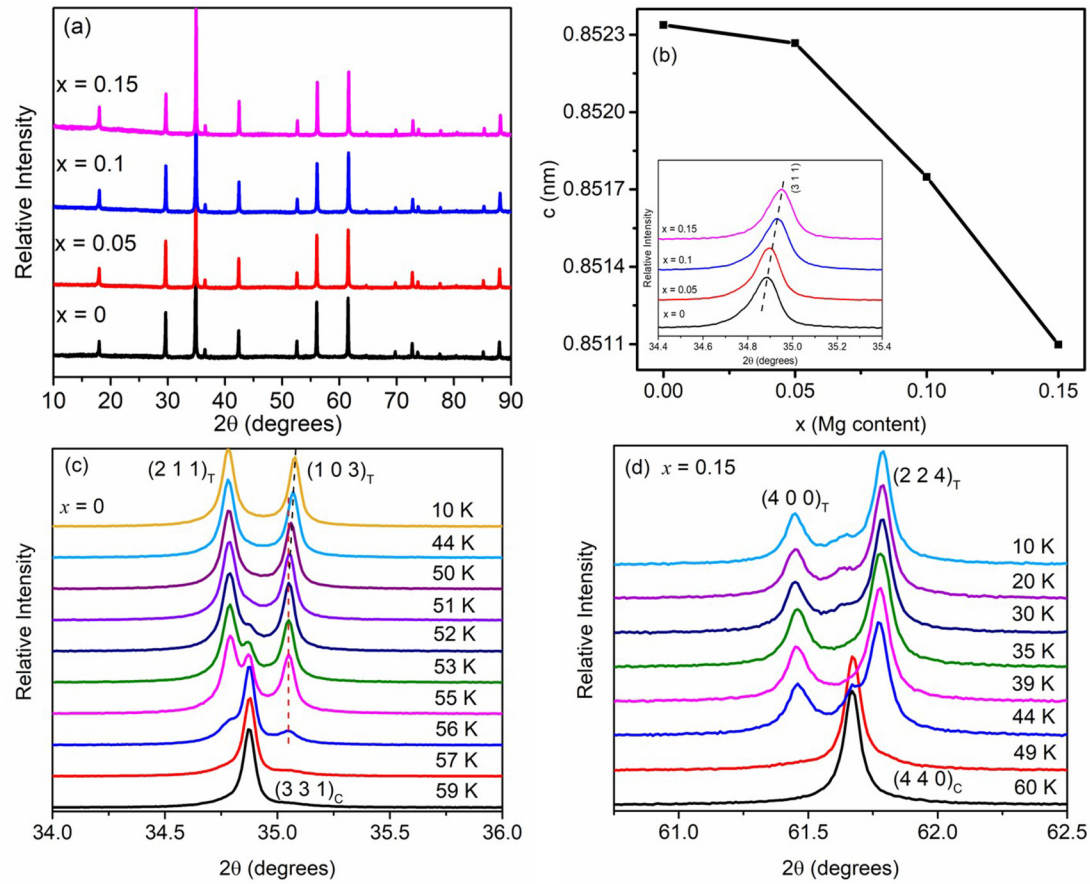

FIG. 1. (a), (b) The powder x-ray-diffraction patterns and lattice parameters for $Mn_{1-x}Mg_xV_2O_4$ ($x = 0$, 0.05, 0.1, 0.15) single crystals at room temperature. The inset in Fig. 1(b) displays the $(311)_C$ diffraction peaks of all samples. (c), (d) The variation temperature XRD patterns around the $(311)_C$ peak for $x = 0$ and around the $(440)_C$ peak for $x = 0.15$, respectively.

Since the distance between V^{3+} ions ($R_{V\text{-}V}$) can be changed by doping M^{2+} ion on the A site [28], the orbital ordering of MnV_2O_4 can be manipulated by the substitution of Mg for Mn. Therefore, we systematically studied the evolution of the magnetic and structural transitions in $Mn_{1-x}Mg_xV_2O_4$ ($x = 0$, 0.05, 0.1, 0.15) single crystals, which all exhibit a cubic-to-tetragonal structural transition at T_S, a ferrimagnetic ordering transition at T_M, and another transition at T^*. The structural transition at T_S is caused by the orbital ordering of V^{3+} ions, but a certain degree of orbital fluctuations arises below T_M due to the special magnetic interactions between V^{3+} ions, which can be suppressed at T^*. Moreover, with increasing Mg doping, the orbital fluctuations are enhanced gradually in $Mn_{1-x}Mg_xV_2O_4$, and the magnetic ordering transition temperature T_M was shifted to lower temperatures, which can be separated clearly from the structural transition at T_S for $x = 0.15$.

II. EXPERIMENT

Appropriate proportions of MnO, MgO, and V_2O_3 were mixed, ground together, and pressed into rods under 120-MPa hydrostatic pressure. Then the rods were calcined at 950 °C for 24 h in an evacuated sealed quartz tube. The single crystals of $Mn_{1-x}Mg_xV_2O_4$ ($x = 0$, 0.05, 0.1, 0.15) were grown by the optical floating-zone technique in pure argon atmosphere, and the feed and seed rods rotate in opposite directions at 25 rpm during crystal growth at a rate of 14 mm/h. Small pieces of single crystal were ground into fine powder to check the phase purity and structural transition at low temperature by XRD. The temperature dependences of magnetic susceptibility $M(T)$ for $Mn_{1-x}Mg_xV_2O_4$ ($x = 0$, 0.05, 0.1, 0.15) crystals with unknown direction were measured under $H = 100$ Oe in zero-field-cooling (ZFC), field-cooled-cooling (FCC), and field-cooled warming (FCW) procedures, performed by the superconducting quantum interference device magnetometer. The measurements of specific heat $C_p(T)$ and thermal conductivity $\kappa(T)$ were performed by the physical property measurement system.

III. RESULTS AND DISCUSSION

As displayed in Figs. 1(a) and 1(b), the $Mn_{1-x}Mg_xV_2O_4$ ($x = 0$, 0.05, 0.1, 0.15) crystals all crystallize in the normal spinel structure with space group $Fd\text{-}3m$ at room temperature, and the lattice parameter a obtained from the Rietveld refinements shows a monotonic reduction with increasing Mg content because the ionic radius of Mg^{2+} ion (0.71 Å) is smaller than that of Mn^{2+} ion (0.80 Å). The low-temperature XRD patterns for $x = 0$ shown in Fig. 1(c) provide clear evidence for a cubic-to-tetragonal structural transition at $T_S = 56$ K due to the splitting of the $(311)_C$ peak into the $(103)_T$

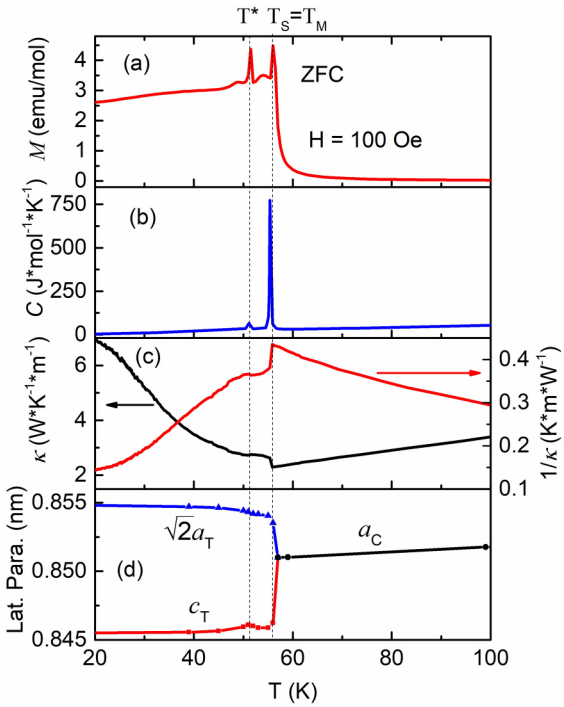

FIG. 2. (a)–(d) The temperature dependences of magnetic susceptibility, specific heat, thermal conductivity, and lattice parameter for MnV_2O_4, respectively.

and $(211)_T$ peaks. Similar to that reported by Zhou *et al.* for pure MnV_2O_4 [16], these patterns also show the coexistence of tetragonal and cubic phase in a narrow temperature range between 52 and 56 K. In addition, these crystals for $x = 0.05$, 0.10, and 0.15 also all exhibit a cubic-to-tetragonal structural transition, whose temperature lowers gradually with increasing x, as shown in Fig. 1(d) and Figs. 1(a) and 1(b) of Supplemental Material [29].

Figures 2(a)–2(d) show the temperature dependences of magnetic susceptibility $M(T)$, specific heat $C_p(T)$, thermal conductivity $\kappa(T)$, and lattice parameters for $x = 0$, respectively. All measurement data display two obvious transitions at the same temperatures ($T_S \sim 56$ K and $T^* \sim 51$ K). The transition at ~56 K has been confirmed to be a cubic-to-tetragonal structural transition by XRD patterns in Fig. 1(c), and the lattice parameter c_T in tetragonal phase shows a maximum value at $T^* \sim 51$ K, indicating an abnormal lattice distortion at T^*. Corresponding to that, the $(103)_T$ peak moves to the left above T^* and to the right below T^* with decreasing temperature, as shown in Fig. 1(c). The $M(T)$ increases rapidly at T_S, suggesting a ferrimagnetic ordering accompanied with the structure transition, which also causes a sharp specific-heat peak at T_S. The second magnetic transition occurs at T^*, where there is a distinct peak in $M(T)$ curve and a weak specific-heat peak. It is impossible to be a transition from collinear to noncollinear ferrimagnetism since the saturation magnetization above and below T^* are the same as shown in Fig. 2 of Supplemental Material [29]. Though its origin is still unclear, the simultaneous appearance of abnormal lattice distortion and magnetic transition suggests a strong spin-lattice coupling at T^*.

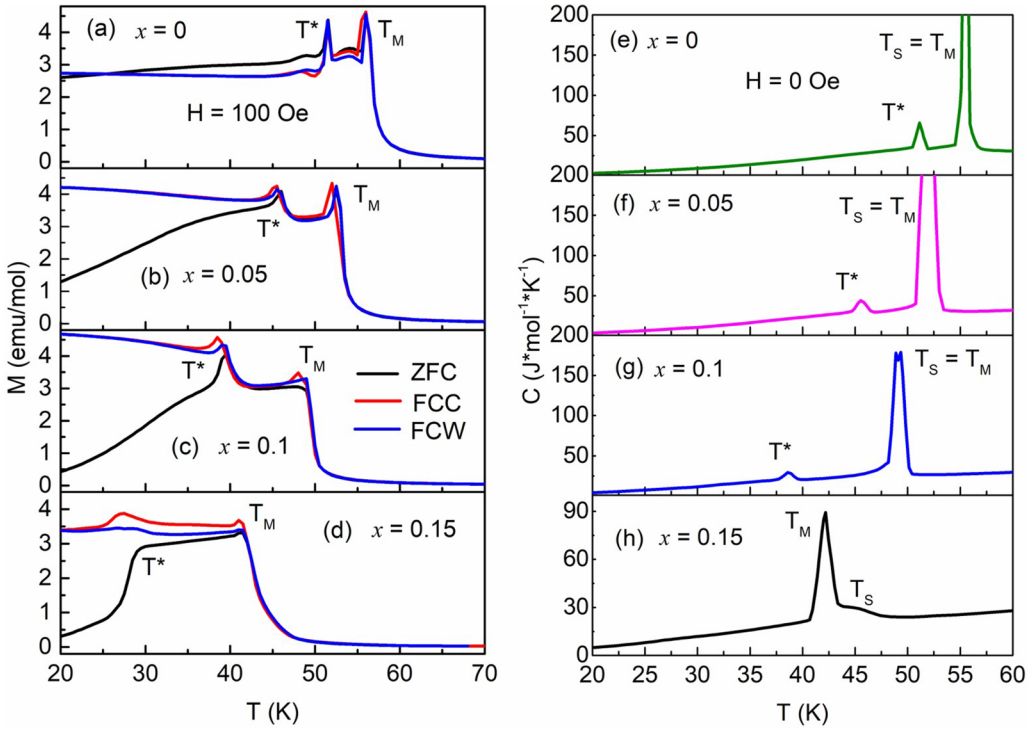

FIG. 3. (a)–(d) The temperature dependences of magnetic susceptibilities for $Mn_{1-x}Mg_xV_2O_4$ single crystals with unknown direction under $H = 100$ Oe in zero-field-cooling (ZFC), field-cooled-cooling (FCC), and field-cooled warming (FCW) procedures. (a) $x = 0$, (b) $x = 0.05$, (c) $x = 0.1$, (d) $x = 0.15$. (e)–(h) The specific heats for $Mn_{1-x}Mg_xV_2O_4$ single crystals under zero field. (e) $x = 0$, (f) $x = 0.05$, (g) $x = 0.1$, (h) $x = 0.15$.

As shown in Fig. 2(c), the negative temperature dependence of $1/\kappa$ above T_S reflects the strong scattering of phonons by disordered orbital [16]. At T_S, a steplike drop observed in the $\kappa(T)^{-1}$ curve indicates that an orbital ordering transition occurs at T_S. The $\kappa(T)^{-1}$ decreases slowly with lowering temperature between T_S and T^*, but the slope increases obviously below T^*, which maybe manifest that the phonon thermal conductivity is only partially restored at T_S and it is further recovered at T^*. Ishitsuka *et al.* reported that the thermal conductivities of AV_2O_4 (A = Mn, Fe, Co) are dominated by the fluctuations of the t_{2g} orbitals of V^{3+} [26,27]. The obvious slope change of $\kappa(T)^{-1}$ suggests that the transition at T^* maybe relate to the change of orbital state. Therefore, we can conclude that the cubic-to-tetragonal structure transition, ferrimagnetic ordering transition, and orbital ordering occur simultaneously at T_S for MnV_2O_4, and the transition at T^* is associated with coupling among the orbital, spin, and lattice degrees of freedom.

For understanding the transition at T^*, we further analyzed the orbital ordering form in MnV_2O_4. Suzuki *et al.* proposed that MnV_2O_4 has an A-type antiferro-orbital ordering, in which d_{yz} and d_{zx} orbitals form a chain along the [110] and the [$\bar{1}$10] directions, respectively, and both are alternately aligned along the c-axis [7]. According to the Goodenough-Kanamori rule, the A-type antiferro-orbital ordering would yield a strong intrachain antiferromagnetic interaction J^{ab} along the d_{yz} and d_{zx} orbital chains and a weak interchain ferromagnetic interaction J^c due to the inappreciable overlap between neighboring d_{yz} and d_{zx}. However, Chung *et al.* observed a large $J^c \sim 3.0$ meV by neutron scattering, meaning a strong antiferromagnetic interaction in MnV_2O_4 [21], which is inconsistent with the Goodenough-Kanamori rule. Moreover, except MnV_2O_4, the J^c of other AV_2O_4 (A = Mg, Mn, Co, Fe, Zn) are all negative [2,11,30,31]. Thus, the anomalous J^c indicates that the A-type antiferro-orbital ordering may be unstable in MnV_2O_4. Therefore, it is possible that a certain degree of orbital fluctuations may exist in MnV_2O_4 below the orbital ordering temperature T_S, and the orbital state of MnV_2O_4 can be further ordered below T^*, leading to the transition at T^*.

In order to verify our speculation about the transition at T^*, we further studied the $Mn_{1-x}Mg_xV_2O_4$ ($x = 0.05$, 0.1, 0.15) crystals, in which the J^c can be adjusted by the change of lattice parameter. The temperature dependences of magnetic susceptibility $M(T)$ and specific heat $C_p(T)$ for $Mg_xMn_{1-x}V_2O_4$ ($x = 0$, 0.05, 0.1, 0.15) crystals are displayed in Figs. 3(a)–3(d) and 3(e)–3(h), respectively. All samples exhibit two significant magnetic transitions with clear thermal hysteresis at low temperature, marked as T_M and T^*, suggesting that they are first-order transitions. Except for $x = 0.15$, the $Mn_{1-x}Mg_xV_2O_4$ ($x = 0$, 0.05, 0.1) crystals all show two specific heat peaks at the same temperatures obtained in the $M(T)$ measurements. With increasing Mg concentration, the transition temperatures T_M and T^* are lowered progressively, and the magnitude of specific-heat peak at T^* is also suppressed gradually and completely disappears for $x = 0.15$. Moreover, besides the sharp peak at $T_M \sim 42$ K, there is still a shoulder at ~46.5 K in the $C_p(T)$ curve for $x = 0.15$. From Fig. 1(d), it can be seen that the $x = 0.15$ sample has a cubic phase at 49 K, but a tetragonal phase at

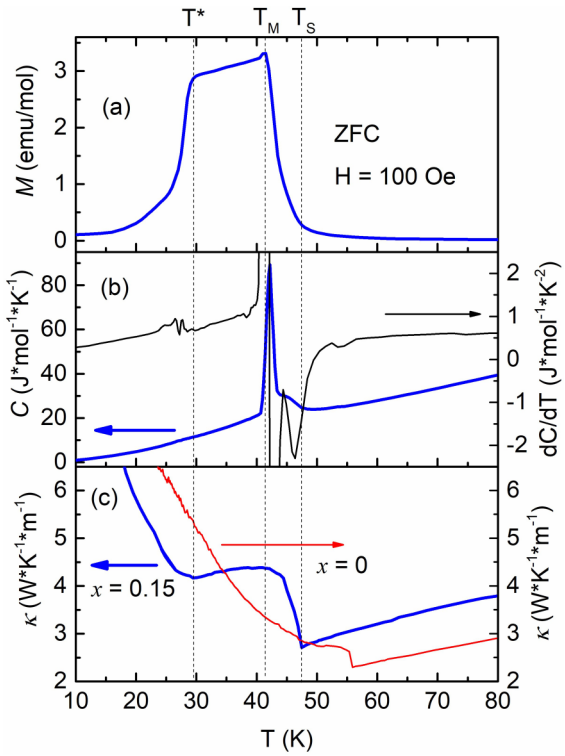

FIG. 4. (a) The variable-temperature magnetic susceptibility for $x = 0.15$. (b) The thick blue line is the specific heat $C_p(T)$ and the thin black line is the derivative of specific heat with respect to temperature $dC_p(T)/dT$. (c) The thermal conductivity for $x = 0.15$ (the thick blue line) and $x = 0$ (the thin red line).

44 K. Considering that the ferrimagnetic ordering occurs at ~42 K in $M(T)$ curve for $x = 0.15$, it can be concluded that the structural transition should take place at $T_S \sim 46.5$ K. These results indicate that the structure transition and ferrimagnetic transition are separated clearly by doping 15% Mg at Mn sites.

As shown in Fig. 4, besides the ferrimagnetic transition at T_M, the $dC_p(T)/dT$ for $x = 0.15$ also displays a sharp minimum at ~46.5 K, indicating a structure transition, and a small kink at ~27.5 K, which is approximately consistent with the T^* in $M(T)$ curve, though there is no obvious abnormality in the $C_p(T)$ curve. Moreover, the jumping temperature in $\kappa(T)$ is higher than the magnetic ordering temperature T_M in $M(T)$, but close to the transition temperature T_S obtained by lattice parameters and $dC_p(T)/dT$ curve, which proves again that the structure transition induced by orbital ordering occurs before the ferrimagnetic transition for $x = 0.15$. With decreasing temperature, the $\kappa(T)$ first increases slowly above T_M, but turns to decrease between T_M and T^*, showing the suppression of phonon thermal conductivity due to the existence of strong orbital fluctuations below T_M. With further decreasing temperature, the phonon thermal conductivity restores partially below T^* for $x = 0.15$, indicating again that the nature of the transition at T^* may be related to the transition from orbital fluctuations to orbital ordering. Though it can be seen from Figs. 1(c) and 1(d) that there is a small amount of cubic phase coexisting with main tetragonal phase below T_S, we still rule out the possibility that the orbital fluctuations are caused by the mixing of orbital disordered

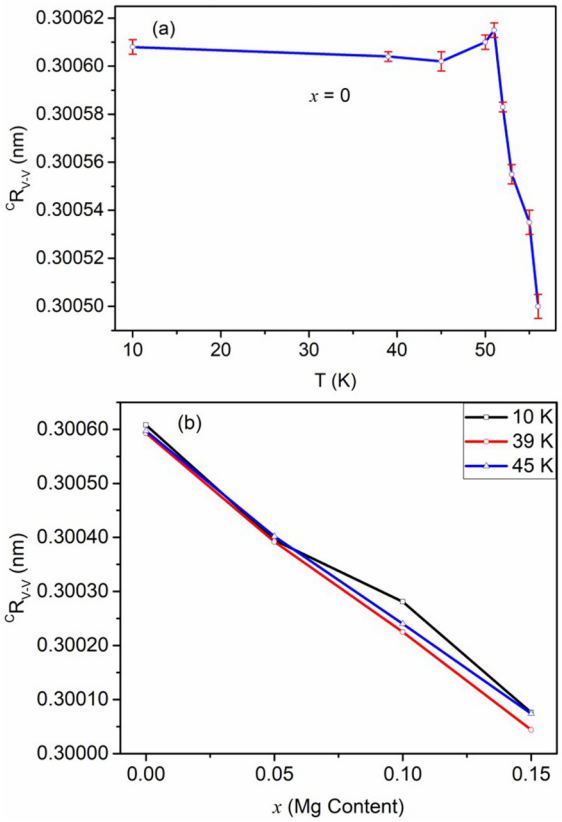

FIG. 5. (a) The temperature dependence of $^cR_{\text{v-v}}$ for $x = 0$. (b) The Mg content dependence of $^cR_{\text{v-v}}$ in tetragonal phase at 10, 39, and 45 K.

cubic phase based on the following two points. First, the orbital fluctuations still exist until $T^* \sim 29$ K, but the cubic phase disappears completely at ~39 K, which is much higher than T^*. Second, the orbital fluctuations for $x = 0.15$ occur below T_M instead of T_S. Therefore, it is reasonable to conclude that the orbital fluctuations are caused by magnetic ordering rather than structural transition, because the J^c can only be uniform after forming long-range magnetic ordering and then leading to the orbital fluctuations below T_M.

Because the orbital fluctuations are dominated by the anomalous large J^c, and the value of $^cR_{\text{v-v}}$ directly influences the overlap between neighboring d_{yz} and d_{zx} orbitals, the smaller $^cR_{\text{v-v}}$, the larger J^c, and the stronger orbital fluctuations. The variations of $^cR_{\text{v-v}}$ (the distance between V^{3+} ions along the c axis) obtained from the a and c lattice parameters in the tetragonal phase are displayed in Fig. 5. The $^cR_{\text{v-v}}$ increases rapidly with decreasing temperature for $x = 0$ between T_S and T^*, suggesting that orbital fluctuations are suppressed gradually with lowering temperature above T^* and the further orbital ordering occurs at T^*. Furthermore, the $^cR_{\text{v-v}}$ in $Mn_{1-x}Mg_xV_2O_4$ solid solution at the same temperature decreases gradually with increasing Mg doping, as shown in Fig. 5(b). Thus, the J^c would gradually increase, leading to the enhancement of orbital fluctuations.

Considering that the Mg has a smaller atomic mass than Mn, replacing Mn by Mg would increase the thermal conductivity of MnV_2O_4, just as shown above T_S. However, we note that the thermal conductivity for $x = 0.15$ is smaller than that for $x = 0$ below T^*. Though the $\kappa(T)$ increases upon decreasing temperature below T^*, the smaller value of $\kappa(T)$ indicates that phonon thermal conductivity is not completely restored for $x = 0.15$ below T^*, suggesting the presence of orbital fluctuations below T^*. Because the orbital fluctuations are enhanced gradually by doping Mg at Mn sites, the specific-heat peak at T^*, which originates from the reduction of orbital entropy, would monotonically weaken with increasing Mg content and disappears completely for $x = 0.15$.

IV. SUMMARY AND CONCLUSION

In conclusion, we have outlined the evolution of phase transitions in $Mn_{1-x}Mg_xV_2O_4$ ($x = 0$, 0.05, 0.1, 0.15) systems. All crystals show the cubic-to-tetragonal structure transition induced by orbital ordering at T_S, accompanied with the ferrimagnetic ordering transition. However, the abnormal large interchain interaction J^c disturbs the orbital ordering and causes a certain degree of orbital fluctuations below $T_M \sim T_S$. With decreasing temperature, the increasing $^cR_{\text{v-v}}$ reduces J^c, which suppresses the orbital fluctuations and further promotes the orbital ordering below T^*. The orbital fluctuations are enhanced by the substitution of Mg on Mn sites due to the increase of $^cR_{\text{v-v}}$. Simultaneously, the ferrimagnetic ordering temperature T_M is also reduced by Mg doping and can be separated clearly from structural transition temperature T_S for $x = 0.15$.

ACKNOWLEDGMENTS

This work is supported by the Natural Science Foundation of China (Grant No. 51472064). J.-G.C. acknowledges the support from MOST, NSFC, and CAS through projects (Grants No. 2018YFA0305700, No. 11574377, No. 11834016, No. 11874400, and No. QYZDBSSW-SLH013).

[1] P. G. Radaelli, New J. Phys. **7**, 53 (2005).
[2] S. H. Lee, D. Louca, H. Ueda, S. Park, T. J. Sato, M. Isobe, Y. Ueda, S. Rosenkranz, P. Zschack, J. Íñiguez, Y. Qiu, and R. Osborn, Phys. Rev. Lett. **93**, 156407 (2004).
[3] J. H. Lee, J. Ma, S. E. Hahn, H. B. Cao, M. Lee, T. Hong, H.-J. Lee, M. S. Yeom, S. Okamoto, H. D. Zhou, M. Matsuda, and R. S. Fishman, Sci. Rep. **7**, 17129 (2017).
[4] G. Giovannetti, A. Stroppa, S. Picozzi, D. Baldomir, V. Pardo, S. Blanco-Canosa, F. Rivadulla, S. Jodlauk, D. Niermann, J. Rohrkamp, T. Lorenz, S. Streltsov, D. I. Khomskii, and J. Hemberger, Phys. Rev. B **83**, 060402(R) (2011).
[5] H. Tsunetsugu and Y. Motome, Phys. Rev. B **68**, 060405(R) (2003).
[6] E. M. Wheeler, B. Lake, A. T. M. Nazmul Islam, M. Reehuis, P. Steffens, T. Guidi, and A. H. Hill, Phys. Rev. B **82**, 140406(R) (2010).
[7] T. Suzuki, M. Katsumura, K. Taniguchi, T. Arima, and T. Katsufuji, Phys. Rev. Lett. **98**, 127203 (2007).

[8] S. Sarkar and T. Saha-Dasgupta, Phys. Rev. B **84**, 235112 (2011).
[9] S. Niitaka, H. Ohsumi, K. Sugimoto, S. Lee, Y. Oshima, K. Kato, D. Hashizume, T. Arima, M. Takata, and H. Takagi, Phys. Rev. Lett. **111**, 267201 (2013).
[10] Y. Nii, H. Sagayama, T. Arima, S. Aoyagi, R. Sakai, S. Maki, E. Nishibori, H. Sawa, K. Sugimoto, H. Ohsumi, and M. Takata, Phys. Rev. B **86**, 125142 (2012).
[11] J. Ma, J. H. Lee, S. E. Hahn, T. Hong, H. B. Cao, A. A. Aczel, Z. L. Dun, M. B. Stone, W. Tian, Y. Qiu, J. R. D. Copley, H. D. Zhou, R. S. Fishman, and M. Matsuda, Phys. Rev. B **91**, 020407(R) (2015).
[12] H. Ishibashi, S. Shimono, K. Tomiyasu, S. Lee, S. Kawaguchi, H. Iwane, H. Nakao, S. Torii, T. Kamiyama, and Y. Kubota, Phys. Rev. B **96**, 144424 (2017).
[13] T. Katsufuji, T. Suzuki, H. Takei, M. Shingu, K. KatoA, K. Osaka, M. Takata, H. Sagayama, and T. H. Arima, J. Phys. Soc. Jpn. **77**, 053708 (2011).
[14] K. Myung-Whun, J. S. Kim, T. Katsufuji, and R. K. Kremer, Phys. Rev. B **83**, 024403 (2011).
[15] K. Adachi, T. Suzuki, K. Kato, K. Osaka, M. Takata, and T. Katsufuji, Phys. Rev. Lett. **95**, 197202 (2005).
[16] H. D. Zhou, J. Lu, and C. R. Wiebe, Phys. Rev. B **76**, 174403 (2007).
[17] V. O. Garlea, R. Jin, D. Mandrus, B. Roessli, Q. Huang, M. Miller, A. J. Schultz, and S. E. Nagler, Phys. Rev. Lett. **100**, 066404 (2008).
[18] V. Hardy, Y. Bréard, and C. Martin, Phys. Rev. B **78**, 024406 (2008).
[19] R. Plumier and M. Sougi, Solid State Commun. **64**, 53 (1987).
[20] Y. J. Huang, Z. Qu, and Y. Zhang, J. Magn. Magn. Mater. **323**, 975 (2011).
[21] D. Choudhury, T. Suzuki, D. Okuyama, D. Morikawa, K. Kato, M. Takata, K. Kobayashi, R. Kumai, H. Nakao, Y. Murakami, M. Bremholm, B. B. Iversen, T. Arima, Y. Tokura, and Y. Taguchi, Phys. Rev. B **89**, 104427 (2014).
[22] A. Kiswandhi, J. S. Brooks, J. Lu, J. Whalen, T. Siegrist, and H. D. Zhou, Phys. Rev. B **84**, 205138 (2011).
[23] X. Luo, Y. P. Sun, W. J. Lu, X. B. Zhu, Z. R. Yang, and W. H. Song, Appl. Phys. Lett. **96**, 062506 (2010).
[24] J.-H. Chung, J.-H. Kim, S.-H. Lee, T. J. Sato, T. Suzuki, M. Katsumura, and T. Katsufuji, Phys. Rev. B **77**, 054412 (2008).
[25] J. H. Chung, Y. S. Song, J. H. Kim, T. Suzuki, T. Katsufuji, M. Matsuda, and S. H. Lee, Phys. Rev. B **88**, 094430 (2013).
[26] T. Omura, T. Ishikawa, Y. Ishitsuka, and T. Katsufuji, Phys. Rev. B **86**, 054436 (2012).
[27] Y. Ishitsuka, T. Ishikawa, R. Koborinai, T. Omura, and T. Katsufuji, Phys. Rev. B **90**, 224411 (2014).
[28] A. Kiswandhi, J. Ma, J. S. Brooks, and H. D. Zhou, Phys. Rev. B **90**, 155132 (2014).
[29] See Supplemental Material at http://link.aps.org/supplemental/10.1103/PhysRevB.100.224418 for further information on the variation temperature XRD patterns of x = 0.05 and 0.10, and the isothermal magnetization curve for $x = 0$.
[30] G. J. MacDougall, I. Brodsky, A. A. Aczel, V. O. Garlea, G. E. Granroth, A. D. Christianson, T. Hong, H. D. Zhou, and S. E. Nagler, Phys. Rev. B **89**, 224404 (2014).
[31] D. Reig-i-Plessis, D. Casavant, V. O. Garlea, A. A. Aczel, M. Feygenson, J. Neuefeind, H. D. Zhou, S. E. Nagler, and G. J. MacDougall, Phys. Rev. B **93**, 014437 (2016).